

Quantum resolution limit of long-baseline imaging using distributed entanglement

Isack Padilla,^{1,*} Aqil Sajjad,^{1,2,†} Babak N. Saif,^{3,‡} and Saikat Guha^{1,2,§}

¹College of Optical Sciences, University of Arizona, Tucson AZ 85721

²Department of Electrical and Computer Engineering,

University of Maryland, College Park MD 20742

³NASA Goddard Space Flight Center, 8800 Greenbelt Rd, Greenbelt, MD 20771, USA

It has been shown that shared entanglement between two telescope sites can in principle be used to localize a point source by mimicking the standard phase-scanning interferometer, but without physically bringing the light from the distant telescopes together. In this paper, we show that a receiver that employs spatial-mode sorting at each telescope site, combined with pre-shared entanglement and local quantum operations can be used to mimic the most general multimode interferometer acting on light collected from the telescopes. As an example application to a quantitative passive-imaging problem, we show that the quantum-limited precision of estimating the angular separation between two stars can be attained by an instantiation of the aforesaid entanglement based receiver. We discuss how this entanglement assisted strategy can be used to achieve the quantum-limited precision of any complex quantitative imaging task involving any number of telescopes. We provide a blueprint of this general receiver that involves quantum transduction of starlight into quantum memory banks and spatial mode sorters deployed at each telescope site, and measurements that include optical detection as well as qubit gates and measurements on the quantum memories. We discuss the relative contributions of local mode sorting at telescope sites vis-a-vis distributed entanglement-assisted interferometry, to the overall quantum-limited information about the scene, based on the ratio of the baseline distance to the individual telescope diameter.

I. INTRODUCTION

In recent years, novel techniques inspired by quantum information theory have emerged in the field of super-resolution imaging, a field of study aimed at increasing the resolution of an imaging system by overcoming the Rayleigh criterion present in diffraction-limited systems, described in [1]. One very promising technique in this regard is spatial-mode demultiplexing (SPADE), which involves spatial mode sorting of the light entering the imaging system. The light is thus measured in a non-trivial spatial mode basis instead of direct detection of its raw intensity profile on a standard imaging screen, which amounts to measuring the incoming photons in the position (or a ‘pixel mode’) basis. This approach has received considerable attention in recent years following Tsang *et al.*’s seminal paper on the problem of estimating the separation between two equally bright incoherent point sources [2]. Using the classical and quantum Cramér-Rao bounds, they show that while this problem suffers from Rayleigh’s curse when direct detection is employed, a measurement in the image-plane Hermite-Gauss (HG) basis when we have a Gaussian point spread function (PSF), can bypass this limit and attain the optimal estimation precision allowed by the laws of physics which is given by the so-called quantum Fisher Information (QFI). This result was generalized to arbitrary aperture shapes by Kerviche *et al.* [3] and Rehacek *et*

al. [4] who independently showed that an optimal SPADE basis for the two equally bright point separation problem can be generated by taking derivatives of increasing orders of the point spread function (PSF) and then performing a Gram-Schmidt orthogonalization process. This yields the sinc-bessel modes for a hard aperture in one dimension. More theory on this has been developed in [2, 5–8], such as extending this to two and three dimensions. Other works have considered estimation of multiple parameters in a scene [9–13], size estimation of extended objects [14, 15], moment estimation of arbitrary scenes [7, 16, 17], object discrimination [18–20], adaptively estimating the locations and brightnesses of several point sources of light [21–23], finding the precise location of an extended object or an array of point sources [24], or estimating different parameters in two stages such as first finding the centroid (i.e., average position) and then the separation between two points [2, 25].

These developments have also inspired some works on the application of quantum information theory techniques to the use of multiple optical receivers or apertures to perform long-baseline interferometry [26–29]. Such a collection of telescopes roughly emulates a single giant telescope with a size equal to the largest distance (baseline) between two nodes of the array, and its working principle consists of interferometrically exploiting the path-length difference of light arriving at two different observation points [30–32]. In such a receiver, information can be extracted in two ways in principle. There is the information contained in the path difference between the light collected at different sites, and then there is also spatial resolution residing in the multi-spatial-mode light collected by each telescope. While most of the works in this field from a quantum information the-

* iacpad0795@arizona.edu

† asajjad@umd.edu

‡ babak.n.saif@nasa.gov

§ saikat@umd.edu

ory point of view have focused on the former alone and mostly taken individual receivers to be small, both effects have been considered in full detail in [29], as the first such treatment. They discuss three broad sets of approaches for combining the light collected by different telescopes. First, when the telescopes are close to, e.g., within a few meters of, one another, we can use at each site a carved out piece of a giant parabola spanning the entire baseline, and focus the light on to a common imaging screen where it can be measured. For larger distances where this is not feasible, we can use a spatial mode sorter at each site, couple the individual local first-few orders of information-rich orthogonal spatial modes into single mode fibers (SMFs), bring them to a central location, process them in a linear interferometer, and measure the outputs with shot-noise-limited photon detectors. This is mathematically equivalent to carrying out a spatial mode measurement on a (hypothetical) giant imaging screen spanning the entire baseline [29]. A related mathematically-equivalent possibility is to employ multi-spatial-mode ‘light pipes’ or vacuum beam guides [33] that carry the entire multi-mode light from each telescope to a central location, feed them into a linear interferometer made of bulk elements (e.g., beam splitters) that preserve the multi-spatial-mode information, and measure the outputs of the interferometer after spatial mode sorting at each output. One could use the light-pipe based interferometric receiver as above, but use bucket detectors at each output of the interferometer rather than spatial-mode-resolved detection. Such a strategy would reap the benefit of the baseline, but not extract scene information contained in local high-order spatial modes.

Both approaches, i.e., using either single mode fibers or light pipes, become challenging to realize for baselines beyond a few hundred meters. Losses in single-mode fiber (for the fiber approach) and accurately transporting the multimode light without distortion and loss (for the light pipe approach) become prohibitive, not to mention the physical impracticality of laying light pipes over large geographical distances through oceans, mountains and other forms of complicated terrain. For larger distances, to attain the fundamental resolution precision afforded by a long baseline system, the alternative is to rely on the (future) *quantum internet*—built using quantum repeaters and satellite-assisted links—that delivers error-corrected high-fidelity entanglement at high rates among the telescope sites, combined with local spatial-mode-resolved light collection and local interferometric measurements at each telescope site.

The simplest example that brings to light the aforesaid issues of quantum limit of a long baseline system, while quantifying the information contributions from mode sorting at each site vis-a-vis entanglement based interferometry, is to consider a two telescope set up for the problem of estimating the angular separation between two stars. At each telescope location, we collect K orthogonal spatial modes with the modes indexed $q = 0, \dots, K - 1$

and couple each into single mode fibers (SMFs), e.g., using a free-space-to-fiber coupled multi-plane light conversion (MPLC) mode sorter. Then, for each mode index q , we bring the respective SMFs from the two sites to a central location and interfere them in a 50-50 beam splitter, followed by detecting both outputs (of each of the K beamsplitters), where the outputs of the q -th beam splitter are the sum and difference of the q -th spatial mode signals from the two telescopes. It has been shown in Ref. [29] that in the large K limit, this pairwise interferometric scheme approaches the quantum Fisher information (QFI) limit of precision for estimating the separation between two uniformly bright point sources in one dimension.

In this paper, we describe how such a pairwise measurement scheme can be implemented using shared entanglement in place of single mode fibers and beam splitters by leveraging and building upon: (1) the quantum protocols for long baseline interferometry proposed by [34], (2) its extension to employ solid-state spin-based quantum memories proposed by [35], and (3) modal imaging techniques for super-resolution with a single telescope [36]. We also show how our approach can be generalized to carrying out a measurement on any arbitrary set of linear combinations of the different modes collected by any number of telescopes. This way, in principle, we can build the most general entanglement-based receiver and tackle any parameter estimation in a quantitative imaging problem [23, 29, 37], for a long-baseline system with any number of telescopes.

In the most general case, let us say we have n telescopes indexed $\alpha = 0, \dots, n - 1$ where modes $q = 0, \dots, K - 1$ are collected at each one of them (since it is impossible to collect an infinite number of modes). And we bring these modes to a central location through single mode fibers where they are combined in a linear interferometer with a desired unitary transformation, which will have nK input modes and nK output modes. Such a linear optical interferometer with any arbitrary unitary transformation can be created using a total of $nK(nK - 1)/2$ Mach-Zehnder interferometers (MZIs) [38]. Since a Mach-Zehnder interferometer comprises two 50-50 beam splitters and two phase shifters, a total of $nK(nK - 1)$ 50-50 beam splitters and the same number of (tunable) phase shifters suffice to realize a general linear optical unitary. This means that if we can create the equivalence of the action of a 50-50 beam splitter (acting on a single-photon state spread across the two modes) by using shared entanglement, in principle we can carry out the same protocol $nK(nK - 1)$ times along with the same number of phase transformations to reproduce the effect of an arbitrary beam splitter circuit with shared entanglement, but without co-locating light from the n telescopes. But, that is exactly what Gottesman et al.’s proposal [34] shows how to do.

Therefore, local spatial-mode sorting at each telescope site, locally-applied single-mode phases and entanglement assisted nonlocal realizations of two-mode 50-

50 beamsplitters (see Fig. 1) can be used to compile the most general nonlocal multimode linear-optical pre-detection interferometry, thus helping attain quantum-limited resolution for quantitative imaging problems discussed above, but limited only by the geometry of, and the light collected by the n -telescope baseline.

Before closing this section, we should mention how this paper fits into the overall picture in terms of existing proposals on the use of shared entanglement for baseline astronomy [34, 35, 40–43]. In the pioneering protocol for entanglement-based interferometry proposed by Gottesman *et al.*, they consider the problem of estimating the phase difference between two telescopes sites for an incoming photon. Say we have $n = 2$ sites where we re-label A and B for $\alpha = 0$ and $\alpha = 1$, respectively. A photon arriving from a star will be in the state $(|1_A, 0_B\rangle + e^{i\theta}|0_A, 1_B\rangle)/\sqrt{2}$, where $|1_A, 0_B\rangle$ is the state for the photon arriving at telescope A , and $|0_A, 1_B\rangle$ if it arrives at location B , with θ being a phase difference arising from the path difference for the photon between the two telescopes. This phase will naturally depend on the position of the star and the distance between the two telescopes, and therefore, in concrete terms, estimating θ amounts to determining the unknown location of a star emitting monochromatic light. In traditional baseline interferometry, we can estimate θ by bringing the light to a common location through ‘light pipes’, put a tunable phase delay in one of these two signals, feed the two light-pipes into a 50-50 beam splitter, and measure the output intensities. As the tunable phase delay matches θ , one of the two outputs becomes zero with totally destructive interference, and the other output contains all the light. Gottesman *et al.*’s proposal mimics this technique by using pre-shared Bell states in the optical ‘single-rail’ basis, i.e., $(|0, 1\rangle + |1, 0\rangle)/\sqrt{2}$, which can be generated by splitting a single photon in a 50-50 beamsplitter, distributed between the telescopes sites reliably via quantum repeaters, local interferometric measurements at each telescope site, and a tunable phase at one telescope site. The main limitation of this scheme is that this entanglement must be provided at an unfeasible rate with the technology available today, and that known repeater architectures—including all-photonic ones [44]—do not deliver photonic Bell states in the single-rail basis suitable for the aforesaid direct local interferometric measurements. Alternative approaches [35, 41, 45] to phase estimation utilize atomic spin memories in cavities assisted with a binary code to logarithmically compress the required number of pre-shared Bell states. This results in exponentially decreased resource requirements compared to the previous proposal in [34], as well as natural compatibility with atomic-qubit-based quantum repeater architectures [46–49].

While these contributions have nicely laid down the ground work for entanglement based interferometry, phase estimation between two sites only allows us to estimate the position of a single object. Moreover, a recent suite of work on quantitative passive imaging shows that

single-source localization is not a good proxy for imaging more complex scene features, and that most photon efficient schemes must involve multimode, potentially adaptive, interferometry prior to detection [23, 37]. In order to carry out more complex quantitative imaging and/or parameter estimation tasks, we need to be able to create an entanglement based equivalent of the conventional multiple telescope interferometric receiver where all the light received at different sites is brought through single mode fibers or ‘light pipes’ to a central location, and fed into a linear interferometer whose outputs are then measured for the number of photon clicks. In Ref. [50], we studied different alternatives of performing this and to create the entanglement-based equivalent of any multiple telescope receiver with spatial mode sorting.

The paper is organized as follows. In Section II, we explain our physical set up with two telescopes and two uniformly bright point sources. In Section III, we write down the joint quantum state of the incoming light. We then dive into our protocol in Section IV, where the first step is to encode the state of the incoming photons at each telescope site on to memory qubits with the above-mentioned logarithmic compression. In Section V, we explain the decoding step where we carry out the measurements to determine the state of an incoming photon in terms of the combinations of the spatial modes collected at both sites. In Section VI, we discuss how this approach attains the quantum limit of performance for the uniformly bright two-point separation problem. Section VII discusses how our protocol generalizes to any arbitrary measurement with any number of apertures. In Section VIII, we conclude the paper with discussions pertaining to future work.

II. OUR PHYSICAL SET-UP

We consider the following set-up: we want to resolve two thermal light emitters, and assume them to be monochromatic and of equal brightness. Our array consists of two telescopes labeled as systems A and B , respectively. For convenience, let us label these systems with $\alpha \in \{A, B\}$. Each site has an aperture that we assume to be symmetrically positioned in the aperture plane. In the case of imaging sources emitting light in optical frequencies (from UV to IR), the incoming light can be modeled as a weak field. Under this assumption, we can model the incoming light as single-rail (absence or presence of a photon) qubit states among the telescope sites, i.e., at a given site, we either have one photon or none. Now, it is convenient to set a measuring time T and subdivide it into M equal intervals of duration $t = T/M$. We can take the probability of detecting a single photon in our two telescope system in each temporal mode (i.e. interval) to be ϵ . The state of a single photon coming in will be a superposition of the states where it arrives at either of the telescopes. One implication of the scheme from [35] being adopted here is that it is only able to

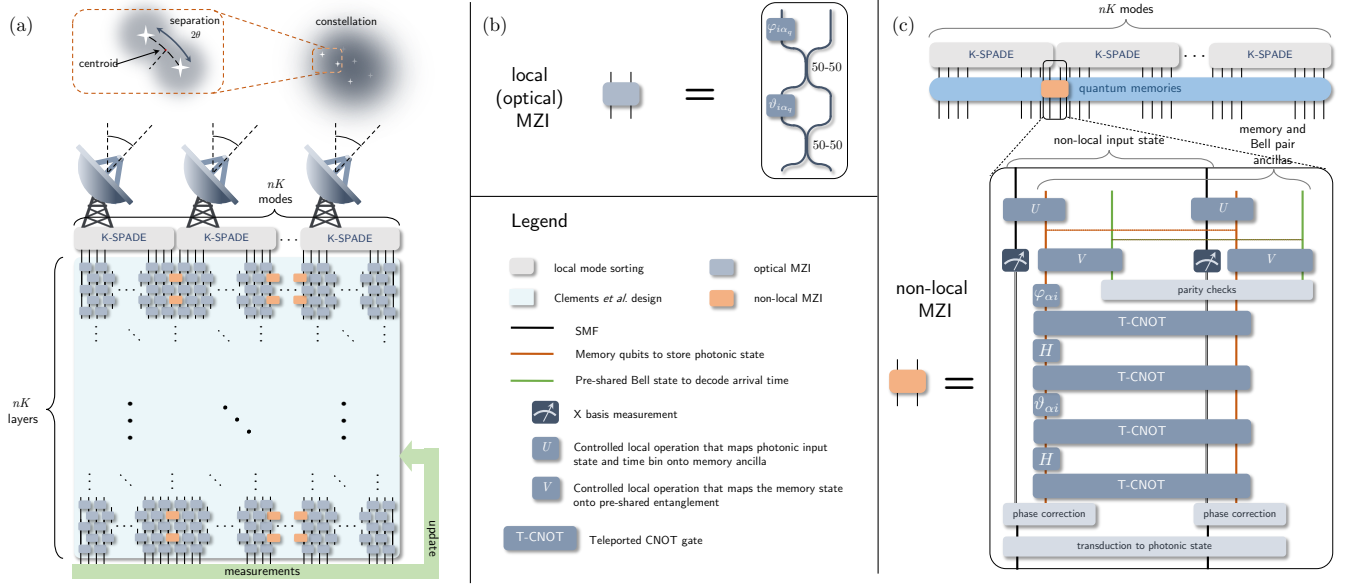


FIG. 1. Overview of the array: Light is being collected at n telescope sites. Each telescope employs a K-ary SPADE which decomposes an incoming signal into K spatial modes in a given basis. The light is then fed into an array of Mach-Zehnder interferometers (MZI), where each contain two phases $\vartheta_{\alpha i}$ and $\varphi_{\alpha i}$, with $i \in \{1, \dots, nK\}$, $\alpha \in \{0, \dots, n-1\}$ and $q \in \{0, \dots, K-1\}$. In total, there are $nK(nK-1)/2$ MZIs. (b) The gray boxes represent an all optical MZI built with two 50-50 beamsplitters. (c) The orange box represents a non-local MZI that employs quantum memories that are use to create entanglement between two sites using a unitary U and Bell pairs to decode the arrival using a unitary V and then perform parity checks time, allowing for better resource expenditure. In order to implement a non-local beamsplitter mimicking transformation, teleported CNOT gates among two nodes can be used [39].

encode a single photon during the integration time with an approximate number of time bins $M \approx 1/\epsilon$. It is then desirable to apply such protocol N times to collect N photons in the ideal scenario. By employing a SPADE at each receiver site and pointing it to the average position known as the centroid, we can take the sources to be located at $\pm\theta$ in the object plane (see Fig. 2). For this, we require prior knowledge of the centroid, which can be achieved reasonably accurately by employing direct detection [2, 24, 25]. Our goal is to estimate θ as accurately as possible within the quantum limit [51]. This can be achieved by measuring the one-photon signal to be in the symmetric or anti-symmetric combinations of each spatial mode at the two telescope sites [29] by employing shared entanglement. More explicitly, such a set-up would thus measure the light entering the two-aperture system in the basis

$$|\phi_{AB,q}^{\pm}\rangle = \frac{1}{\sqrt{2}} (|1_{A_q}, 0_B\rangle \pm |0_A, 1_{B_q}\rangle), \quad q = 0, \dots, \infty \quad (1)$$

where in a nutshell, $|1_{A_q}, 0_B\rangle$ and $|0_A, 1_{B_q}\rangle$ are the kets associated with a single photon in mode q at sites A and B , respectively, and we will make this notation more precise later.

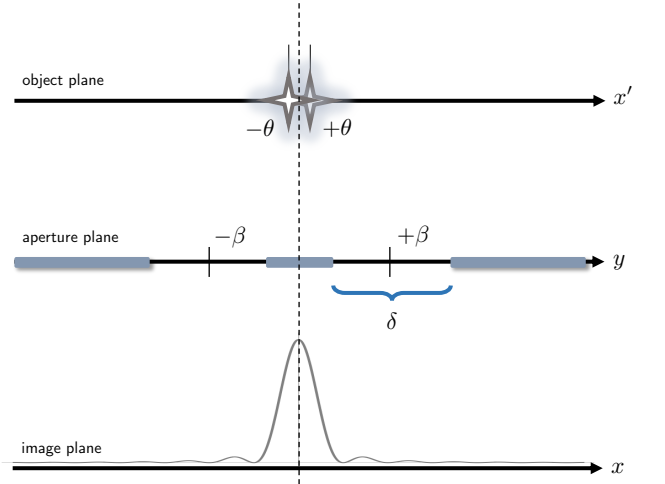


FIG. 2. Schematic showing light originating at object plane, propagating until reaching aperture plane, with $n = 2$ hard apertures of size δ , and finally producing an image at image plane.

III. JOINT QUANTUM STATE OF THE COLLECTED LIGHT

We will do this in three steps. First we write the quantum state for a single time bin for just one telescope. We will then give the generalization to two telescopes, and finally, we will write down the full quantum state for multiple time bins.

A. The single-aperture case

We take the probability of a single incoming photon in a given temporal mode to be ϵ [2]. The density operator for a thermal source, weak enough to only consider linear terms after expanding in ϵ , is

$$\rho = (1 - \epsilon)\rho_0 + \epsilon\rho_1, \quad (2)$$

where $\rho_0 = |0\rangle\langle 0|$ denotes vacuum and the one-photon state is a mixture of states of the incoming light from each star, labeled $s \in \{1, 2\}$:

$$\rho_1 = \frac{1}{2} \sum_{s \in \{1, 2\}} |\psi^{(s)}\rangle \langle \psi^{(s)}|. \quad (3)$$

In the single aperture case, we can write the state for star s as

$$|\psi^{(s)}\rangle = \int dx \psi(x - x_s) |x\rangle, \quad (4)$$

where x is the coordinate over the image-plane, $|x\rangle = a^\dagger(x)|0\rangle$ is the state of a single photon at position x , and $a^\dagger(x)$ the bosonic creation operator in the continuum limit which satisfies the usual commutation relation $[a(x), a^\dagger(x')] = \delta(x - x')$ [52]. Lastly, $\psi(x - x_s)$ is the point-spread function (PSF) corresponding to a single aperture, with x_s being the position of the s -th star in the object plane.

Now, consider sorting light collected by our aperture in terms of spatial mode basis functions $\phi_q(x)$ with $q = 0, 1, 2, \dots$. Expanding the state $|\psi^{(s)}\rangle$ defined in Eq. (4) into such a basis gives

$$|\psi^{(s)}\rangle = \sum_{q=0}^{\infty} \Gamma_q(x_s) |1_q\rangle, \quad (5)$$

where

$$|1_q\rangle = \int dx \phi_q(x) |x\rangle \quad (6)$$

is the ket for a single photon in the modal function $\phi_q(x)$ (and no photons in all the other modes), and the coefficients $\Gamma_q(x_s)$ are defined as the correlation functions between the PSF and the modal functions:

$$\Gamma_q(x_s) = \langle 1_q | \psi^{(s)} \rangle \quad (7)$$

$$= \int dx \phi_q^*(x) \psi(x - x_s). \quad (8)$$

The probability of measuring an incoming photon in the above basis and finding it to be in the q th mode is then given as $p_q(x_s) = |\Gamma_q(x_s)|^2$.

To obtain the PSF, we need to take the Fourier transform of the aperture function $\tilde{\psi}(y)$, where y is the coordinate in the aperture plane. We will consider the realistic scenario of a hard aperture function

$$\tilde{\psi}(y) = \text{rect}(y/\delta) / \sqrt{\delta}, \quad (9)$$

where δ is the size of the aperture. The Fourier transform of this yields the PSF

$$\psi(x) = \sqrt{\sigma} \frac{\sin(\pi x/\sigma)}{\pi x}. \quad (10)$$

where $\sigma = 2\pi/\delta$ is the Rayleigh separation.

While we can measure in any basis, one natural basis set can be constructed by taking the PSF as the fundamental mode, then taking derivatives of it of increasing order, and finally applying a Gram-Schmidt process to obtain the subsequent modes. For the above PSF for a hard aperture in 1 dimension, this results in the Sinc-Bessel (SB) basis, for which the mode functions are $\phi_q(x) \equiv \sqrt{(1+2q)/\sigma} j_q(\pi x/\sigma)$, where $j_q(\pi x/\sigma)$ are the spherical Bessel functions of the first kind [3, 53]. The correlation functions for this basis are

$$\Gamma_q(x_s) = \sqrt{\sigma} \phi_q(x_s) \quad (11)$$

It was in fact shown in [29] that this equation will exactly hold for any modal basis if we have a hard aperture in 1 dimension. For a two-dimensional hard aperture, $\sqrt{\sigma}$ will be replaced by a slightly different constant that is proportional to the square root of the area of the hard apertures. We should however point out that the results and calculations given in this paper are mostly independent of the choice of the modal basis.

B. The state for the two telescope set up

We now consider two apertures at positions $y_A = -\beta$ and $y_B = \beta$ for which we will also use the notation y_α with $\alpha \in \{A, B\}$. We will mostly follow the framework described in [29], which we now summarize, but with slightly modified notation and conventions.

When we have two apertures, the aperture function $\tilde{\psi}(y)$ gets replaced by the normalized sum of two aperture functions centered at the two telescope locations $(\tilde{\psi}(y - y_A) + \tilde{\psi}(y - y_B)) / \sqrt{2}$. Now, imagine a large hypothetical imaging screen behind the two apertures spanning the entire baseline so that the light entering the two hard apertures forms an image on it. The PSF for this is the Fourier transform of this combined aperture function, just as the PSF for a single aperture is obtained by Fourier transforming the single-aperture function. Note that a shift in a function translates into a phase in the Fourier transform. Specifically, the Fourier transform of the shifted single-aperture function $\tilde{\psi}(y - y_\alpha)$ is $e^{-iy_\alpha x} \psi(x)$, where $\psi(x)$ is the single-aperture PSF obtained

by Fourier transforming the unshifted function $\tilde{\psi}(y)$. Applying this to the contributions from both apertures, the combined aperture function is

$$\psi_{2\text{-ap}}(x) = \sqrt{2} \cos(\beta x) \psi(x), \quad (12)$$

that is, the PSF for a single unshifted aperture times a cosine term containing information about the two-aperture system (with $\sqrt{2}$ arising from the normalization. For the special case of two hard, rect shaped apertures with the aperture function (9) centered at positions $\pm\beta$ in the aperture plane, we obtain the combined PSF

$$\psi_{2\text{-ap, h}}(x) = \sqrt{2\sigma} \cos(\beta x) \frac{\sin(\pi x/\sigma)}{\pi x}, \quad (13)$$

We will refer back to this in the last section when we evaluate the performance of the measurement carried out by our protocol.

The quantum state for a single photon originating from a point source at position x_s and entering our two-aperture system is a linear combination of starlight arriving at site A or B

$$\begin{aligned} |\psi_{AB}^{(s)}\rangle &= \int dx \psi_{2\text{-ap}}(x) |x\rangle \\ &= \frac{1}{\sqrt{2}} \left(|\psi_A^{(s)}\rangle + |\psi_B^{(s)}\rangle \right) \end{aligned} \quad (14)$$

where $|x\rangle$ is the position ket for a photon hitting an imaginary imaging screen spanning the entire baseline, and $|\psi_A^{(s)}\rangle$ and $|\psi_B^{(s)}\rangle$ are the kets associated with the photon arriving at the two locations

$$|\psi_\alpha^{(s)}\rangle = \int dx e^{-iy_\alpha(x-x_s)} \psi(x-x_s) |x\rangle, \quad \alpha \in \{A, B\} \quad (15)$$

In the same spirit, the mode functions $\phi_q(x)$ also acquire the same phase factor as $\psi(x)$ when the aperture is shifted to a position y_α . This can be seen by thinking in terms of the aperture plane where $\phi_q(x)$ translates into its Fourier transform $\tilde{\phi}_q(y)$. If the aperture is shifted to a location y_α in the aperture plane, then the mode function becomes $\tilde{\phi}_q(y-y_\alpha)$, which in the image plane gives $\exp(-iy_\alpha x) \phi_q(x)$. We then have the state

$$|1_{A_q}, 0_B\rangle \equiv a_{A_q}^\dagger |0_A, 0_B\rangle = \int dx e^{-iy_A x} \phi_q(x) |x\rangle \quad (16)$$

for a single photon in mode q of the telescope at site A , and

$$|0_A, 1_{B_q}\rangle \equiv a_{B_q}^\dagger |0_A, 0_B\rangle = \int dx e^{-iy_B x} \phi_q(x) |x\rangle \quad (17)$$

for a single photon in mode q at site B . Here $|0_\alpha\rangle \equiv \bigotimes_{i=0}^\infty |0_{\alpha_i}\rangle$ is the vacuum in all the spatial modes at site α , in terms of which our position ket on an imaginary imaging screen spanning the entire baseline is $|x\rangle = a^\dagger(x) |0_A, 0_B\rangle$, and $a_{\alpha_q}^\dagger = \int dx e^{-iy_\alpha x} \phi_q(x) a^\dagger(x)$ is the creation operator for a photon in the q -th mode at site α .

We will refer to $|1_{A_q}, 0_B\rangle$ and $|0_A, 1_{B_q}\rangle$ as the local modes of the telescopes at sites A and B , respectively. The local modes of one aperture will be orthogonal to those of another one, and this has been shown in detail in [29]. Overall, the local modes of all our apertures will provide a complete orthonormal basis for our multiple aperture system.

Having specified how the local mode functions and the PSF acquire phase factors when we shift an aperture from the origin to a position y_α in the aperture plane, we can expand the ket $|\psi_\alpha^{(s)}\rangle$ associated with a photon from a star at position x_s arriving in aperture α in terms of its local modes. From (15), (16) and (17), we obtain

$$\begin{aligned} \langle 1_{A_q}, 0_B | \psi_A^{(s)} \rangle &= e^{iy_A x_s} \Gamma_q(x_s), \text{ and} \\ \langle 0_A, 1_{B_q} | \psi_B^{(s)} \rangle &= e^{iy_B x_s} \Gamma_q(x_s). \end{aligned} \quad (18)$$

Using this result and expanding (14) in terms of the local modes, we obtain

$$\begin{aligned} |\psi_{AB}^{(s)}\rangle &= \frac{1}{\sqrt{2}} \sum_{q=0}^\infty \Gamma_q(x_s) \left(e^{iy_A x_s} |1_{A_q}, 0_B\rangle + e^{iy_B x_s} |0_A, 1_{B_q}\rangle \right) \\ &= \frac{1}{\sqrt{2}} \sum_{q=0}^\infty \Gamma_q(x_s) \left(e^{-i\beta x_s} |1_{A_q}, 0_B\rangle + e^{i\beta x_s} |0_A, 1_{B_q}\rangle \right) \end{aligned} \quad (19)$$

where in the second line, we have plugged in $y_A = -\beta$ and $y_B = \beta$ for the telescope positions.

In a realistic physical set up, we will only be able to collect a finite number of spatial modes at each site. Assuming that we are collecting only the first K modes, this results in the above state being projected on to the subspace limited to $0 \leq q \leq K-1$

$$\begin{aligned} |\psi_{AB}^{(s)}\rangle \rightarrow |\psi_{AB,K}^{(s)}\rangle &\equiv \frac{1}{\sqrt{2}} \sum_{q=0}^{K-1} \eta_q(x_s) \left(e^{-i\beta x_s} |1_{A_q}, 0_B\rangle \right. \\ &\quad \left. + e^{i\beta x_s} |0_A, 1_{B_q}\rangle \right), \end{aligned} \quad (20)$$

where

$$\eta_q(x_s) \equiv \frac{\Gamma_q(x_s)}{\sqrt{\sum_{l=0}^{K-1} \Gamma_l^2(x_s)}} \quad (21)$$

are the new coefficients obtained from dividing $\Gamma_q^2(x_s)$ by the normalization factor $\sqrt{\sum_{l=0}^{K-1} \Gamma_l^2(x_s)}$. However, for a sufficiently large K , this factor will approach 1, and we recover $\eta_q(x_s) \rightarrow \Gamma_q(x_s)$. In the same spirit, the photon flux will also change if we only collect the first K modes, being redefined as

$$N_K \equiv N \sum_{l=0}^{K-1} \Gamma_l^2(x_s), \quad (22)$$

which will approach N for a sufficiently large K for which $\sum_{l=0}^{K-1} \Gamma_l^2(x_s)$ will approach unity.

Our goal is to use shared entanglement to measure the incoming photon in the pairwise basis introduced in [29]

$$|\phi_{AB,q}^\pm\rangle = \frac{1}{\sqrt{2}} \left(|1_{A_q}, 0_B\rangle \pm |0_A, 1_{B_q}\rangle \right) \quad (23)$$

The projection of (20) onto these yield the respective probabilities

$$p_q^\pm = \eta_q^2(x_s) \cos^2(\beta x_s) \quad (24)$$

and

$$p_q^- = \eta_q^2(x_s) \sin^2(\beta x_s), \quad (25)$$

which are the probabilities we want to replicate with the entanglement-based protocol presented here. In the limit where we collect a large number of spatial modes i.e. $K \rightarrow \infty$, these approach $\Gamma_q^2(x_s) \cos^2(\beta x_s)$ and $\Gamma_q^2(x_s) \sin^2(\beta x_s)$, respectively, which are the probabilities obtained in [29].

Having spelled out the ket for a photon originating from a given point source, we can write down the density operator describing the weak incoming signal, arriving at sites A and B

$$\rho_{AB} = (1 - \epsilon)\rho_{0,AB} + \epsilon\rho_{1,AB}, \quad (26)$$

Where $\rho_{0,AB} = |0_A, 0_B\rangle\langle 0_A, 0_B|$ is the vacuum state across both locations which we defined above, and the one-photon state for the two aperture system is a mixture of the one-photon states associated with the two point sources

$$\rho_{1,AB} = \frac{1}{2} \sum_{s \in \{1,2\}} \left| \psi_{AB,K}^{(s)} \right\rangle \left\langle \psi_{AB,K}^{(s)} \right|, \quad (27)$$

where $|\psi_{AB,K}^{(s)}\rangle$ was given in (20).

C. The state over multiple time bins

During the measurement time, the state that describes the incoming light in a given time interval $T = tM$ is $\rho_{AB}^{\otimes M}$, where M is the total number of temporal modes or time bins indexed with $m \in \{1, \dots, M\}$. By computing this tensor product (see Appendix A for a detailed derivation), and keeping only linear terms in ϵ (in order to guarantee the presence of at most one photon over the total measuring time T), we obtain

$$\rho_{AB}^{\otimes M} \approx (1 - M\epsilon)\rho_{0,AB}^{\otimes M} + \epsilon \sum_{m=1}^M \rho_{1,AB,m}, \quad (28)$$

where $\rho_{1,AB,m}$ is a tensor product of M states of which $M-1$ are vacuum and the remaining one is a one-photon state $\rho_{1,AB}$ in the m -th position:

$$\rho_{1,AB,m} = \rho_{0,AB}^{\otimes(m-1)} \otimes \rho_{1,AB} \otimes \rho_{0,AB}^{\otimes(M-m)} \quad (29a)$$

$$= \rho_{0,AB}^{\otimes(m-1)} \otimes \frac{1}{2} \sum_{s \in \{1,2\}} \left| \psi_{AB,K}^{(s)} \right\rangle \left\langle \psi_{AB,K}^{(s)} \right| \otimes \rho_{0,AB}^{\otimes(M-m)} \quad (29b)$$

$$= \frac{1}{2} \sum_{s \in \{1,2\}} \left| \psi_{AB,K,m}^{(s)} \right\rangle \left\langle \psi_{AB,K,m}^{(s)} \right|. \quad (29c)$$

The ket in Eq. (29c) is for a single photon from star s arriving at time bin m defined as

$$\left| \psi_{AB,K,m}^{(s)} \right\rangle \equiv |0_A, 0_B\rangle^{\otimes(m-1)} \otimes \left| \psi_{AB,K}^{(s)} \right\rangle \otimes |0_A, 0_B\rangle^{\otimes(M-m)} \quad (30a)$$

$$= \frac{1}{\sqrt{2}} \sum_{q=0}^{K-1} \eta_q(x_s) \left(e^{i\beta x_s} |0_A, 0_B\rangle^{\otimes(m-1)} \otimes |0_A, 1_{Bq}\rangle \otimes |0_A, 0_B\rangle^{\otimes(M-m)} \right. \\ \left. + e^{-i\beta x_s} |0_A, 0_B\rangle^{\otimes(m-1)} \otimes |1_{Aq}, 0_B\rangle \otimes |0_A, 0_B\rangle^{\otimes(M-m)} \right) \quad (30b)$$

$$= \frac{1}{\sqrt{2}} \sum_{q=0}^{K-1} \eta_q(x_s) \left(e^{i\beta x_s} \left| \tilde{0}_A, \tilde{1}_{Bmq} \right\rangle + e^{-i\beta x_s} \left| \tilde{1}_{Amq}, \tilde{0}_B \right\rangle \right), \quad (30c)$$

where $|\psi_{AB,K}^{(s)}\rangle$ was given in (20), and

$$\left| \tilde{0}_\alpha \right\rangle \equiv \bigotimes_{i=0}^{K-1} \bigotimes_{j=1}^M |0_{\alpha_{ji}}\rangle, \quad \alpha \in \{A, B\} \quad (31)$$

and

$$\left| \tilde{1}_{\alpha mq} \right\rangle = a_{\alpha mq}^\dagger \left| \tilde{0}_\alpha \right\rangle, \quad \alpha \in \{A, B\} \quad (32)$$

are the kets for vacuum across the KM modes and one photon in spatio-temporal mode mq , respectively. The creation operator $a_{\alpha mq}^\dagger$ produces a photon in the mq -th spatio-temporal mode at site α . Since we are only considering zero photon states and single photon excitations, we can think of the state associated with each spatio-temporal mode at a given site as a single rail qubit, which is in $|0\rangle$ if there is no photon, and $|1\rangle$ if there is one photon.

In the next sections, we address the different stages towards interferometry of the incoming photons. First we go through

the encoding process in which starlight information is mapped onto a quantum memory in the fashion of [35, 41]. In the decoding section, we show how the memory is mapped onto ancilla Bell pairs to transfer the information from one of the aperture sites to the other.

IV. ENCODING PHOTONIC QUANTUM STATE INTO QUANTUM MEMORIES

The encoding step involves transferring the state of the photons to a quantum memory state described by sets of systems \bar{A} and \bar{B} , labeled $\bar{\alpha} \in \{\bar{A}, \bar{B}\}$, which start as a register, for a given spatial mode, of $\bar{M} = \log_2(M+1)$ qubits initialized in the state $|0\rangle$. We introduce indices $k \in \{1, \dots, \bar{M}\}$, $i \in \{0, \dots, K-1\}$ and $j \in \{1, \dots, M\}$ that account for the resources used throughout the protocol (memory qubits, CNOT gates and pre-shared Bell pairs, respectively), with the special case $i = q$ and $j = m$ corresponding to the spatio-temporal

mode m_q where the photonic excitation is present. For both sites we write the state of the memory qubits as

$$\sigma_0 = |0_{\bar{A}}, 0_{\bar{B}}\rangle \langle 0_{\bar{A}}, 0_{\bar{B}}|, \quad (33)$$

where we have defined

$$|0_{\bar{\alpha}}\rangle \equiv \bigotimes_{i=0}^{K-1} \bigotimes_{k=1}^{\bar{M}} |0_{\bar{\alpha}_{ki}}\rangle, \quad \alpha \in \{A, B\}, \quad (34)$$

so a total of $2K\bar{M}$ memory qubits are employed.

We then wish to load the photonic state on to the memory qubits. For this purpose, we employ a collection of CNOT gates from the photonic qubits to the memory ones such that a photonic excitation in the i th spatial mode in the j th time bin at a given site translates into excitations in the binary representation of j in the memory qubits corresponding to spatial mode i at the same location. These CNOT operations for site α can be denoted by $U_{\alpha_{ji}, \bar{\alpha}_{ki}}$, where we identify the control and target qubits as the photonic qubit in the i -th spatial mode and j -th temporal mode (photonic qubit α_{ji}) and the k -th qubit in the memory (memory qubit $\bar{\alpha}_{ki}$), respectively. The full operator acting on the state for all spatial and temporal modes at site α is

$$U_{\alpha\bar{\alpha}} = \bigotimes_{i=0}^{K-1} \bigotimes_{j=1}^M \bigotimes_{k=1}^{\bar{M}} (U_{\alpha_{ji}, \bar{\alpha}_{ki}})^{w_{kj}}, \quad \alpha \in \{A, B\} \quad (35)$$

Here the symbol w_{kj} represents the k th digit in the binary form of j ; e.g., if we have a photon in $j = 5$, its binary representation is the bit-string 101, then $w_{15} = 1$, $w_{25} = 0$, $w_{35} = 1$ and $w_{k'5} = 0$ for $k' \in \{4, \dots, \bar{M}\}$.

The action of the CNOTs at each site (35) thus gives

$$U_{\alpha\bar{\alpha}} |\tilde{1}_{\alpha_{mq}}\rangle |0_{\bar{\alpha}}\rangle = |\tilde{1}_{\alpha_{mq}}\rangle |1_{\bar{\alpha}_{mq}}\rangle, \quad \alpha \in \{A, B\} \quad (36)$$

where

$$|1_{\bar{\alpha}_{mq}}\rangle \equiv \bigotimes_{i=0}^{K-1} \bigotimes_{k=1}^{\bar{M}} X_{\bar{\alpha}_{ik}}^{\delta_{iq} w_{km}} |0\rangle_{\bar{\alpha}_{ki}} \quad (37)$$

is the logical representation of the mapped excitation in the memory. Here $X_{\bar{\alpha}_{ik}}$ denotes the Pauli X operator acting on the memory qubit of system $\bar{\alpha}$ corresponding to the k -th memory qubit of spatial mode i , flipping it from $|0\rangle$ into $|1\rangle$.

Now, the combined state of the photon and the blank memory is $\rho_{AB}^{\otimes M} \otimes \sigma_0$, and the encoding is performed by the operator $U \equiv U_{A\bar{A}} \otimes U_{B\bar{B}}$. Then, the photon-memory state after

applying the CNOTs is

$$\rho_{AB\bar{A}\bar{B}} = U \rho_{AB}^{\otimes M} \otimes \sigma_0 U^\dagger \quad (38)$$

$$= (1 - M\epsilon) \rho_{0,AB}^{\otimes M} \otimes \sigma_0 + \frac{\epsilon}{2} \sum_{\substack{m=1 \\ s \in \{1,2\}}}^M |\psi_{AB\bar{A}\bar{B},m}^{(s)}\rangle \langle \psi_{AB\bar{A}\bar{B},m}^{(s)}|, \quad (39)$$

with the following ket obtained after applying the compound CNOT unitary U on the photon and memory states:

$$|\psi_{AB\bar{A}\bar{B},m}^{(s)}\rangle \equiv \frac{1}{\sqrt{2}} \sum_{q=0}^{K-1} \eta_q(x_s) \left(e^{i\beta x_s} |\tilde{0}_A, \tilde{1}_{B_{mq}}\rangle |0_{\bar{A}}, 1_{\bar{B}_{mq}}\rangle + e^{-i\beta x_s} |\tilde{1}_{A_{mq}}, \tilde{0}_B\rangle |1_{\bar{A}_{mq}}, 0_{\bar{B}}\rangle \right). \quad (40)$$

The result from this mapping is thus an entangled state between the photon and the memory. The next step is to disentangle the two and separate the photons from this. This is done by measuring the photonic qubits (systems A and B) in the X basis $|\pm\rangle = (|0\rangle \pm |1\rangle)/\sqrt{2}$. Such measurement of the photonic modes will introduce a conditional phase in the state of the memory qubits. One way we can deal with this is by expanding the photonic portions of (40) into a sum of four X basis tensor product states. First note that going from the Z basis to the X basis for two modes yields the following:

$$|0_{A_{ji}}, 0_{B_{ji}}\rangle = \frac{1}{2} \left(| +_{A_{ji}} +_{B_{ji}} \rangle + | -_{A_{ji}} -_{B_{ji}} \rangle - | +_{A_{ji}} -_{B_{ji}} \rangle + | -_{A_{ji}} +_{B_{ji}} \rangle \right), \quad (41)$$

$$|1_{A_{ji}}, 0_{B_{ji}}\rangle = \frac{1}{2} \left(| +_{A_{ji}} +_{B_{ji}} \rangle - | -_{A_{ji}} -_{B_{ji}} \rangle + | +_{A_{ji}} -_{B_{ji}} \rangle - | -_{A_{ji}} +_{B_{ji}} \rangle \right), \quad (42)$$

$$|0_{A_{ji}}, 1_{B_{ji}}\rangle = \frac{1}{2} \left(| +_{A_{ji}} +_{B_{ji}} \rangle - | -_{A_{ji}} -_{B_{ji}} \rangle - | +_{A_{ji}} -_{B_{ji}} \rangle + | -_{A_{ji}} +_{B_{ji}} \rangle \right). \quad (43)$$

This allows us to re-write the photon-memory state (40) in the form

$$\begin{aligned} |\psi_{AB\bar{A}\bar{B},m}^{(s)}\rangle &= \frac{1}{\sqrt{2}} \sum_{q=0}^{K-1} \eta_q(x_s) |e_{AB,mq}\rangle \left(e^{i\beta x_s} |0_{\bar{A}}, 1_{\bar{B}_{mq}}\rangle + e^{-i\beta x_s} |1_{\bar{A}_{mq}}, 0_{\bar{B}}\rangle \right) \\ &\quad + \frac{1}{\sqrt{2}} \sum_{q=0}^{K-1} \eta_q(x_s) |o_{AB,mq}\rangle \left(e^{i\beta x_s} |0_{\bar{A}}, 1_{\bar{B}_{mq}}\rangle - e^{-i\beta x_s} |1_{\bar{A}_{mq}}, 0_{\bar{B}}\rangle \right), \end{aligned} \quad (44)$$

where

$$|e_{AB,mq}\rangle = \frac{1}{\sqrt{2}} \left(| +_{A_{mq}}, +_{B_{mq}} \rangle - | -_{A_{mq}}, -_{B_{mq}} \rangle \right) \quad (45)$$

and

$$|o_{AB,mq}\rangle = \frac{1}{\sqrt{2}} \left(| -_{A_{mq}}, +_{B_{mq}} \rangle - | +_{A_{mq}}, -_{B_{mq}} \rangle \right) \quad (46)$$

are the ‘‘even’’ and ‘‘odd’’ photonic states, respectively. The kets $|\pm_{\alpha m q}\rangle$ contained in (45) and (46) are the states in which all the photonic qubits are in $|0\rangle$ except the one corresponding to the spatio-temporal mode $m q$, which is in $|\pm\rangle$, at site α . More concisely, we can write such states as $|+\alpha m q\rangle = H_{\alpha m q}|\bar{0}_\alpha\rangle$ and $|-\alpha m q\rangle = Z_{\alpha m q}H_{\alpha m q}|\bar{0}_\alpha\rangle$, where $H_{\alpha m q}$ and $Z_{\alpha m q}$ are the Hadamard and Pauli Z operators acting solely on spatio-temporal mode $m q$ of (31), respectively.

Thus from (44), we see that measuring the photonic qubits in the X basis dis-entangles the photon-memory system, but gives a conditional sign flip in the memory state depending on whether we obtain odd (\pm, \pm) or even (\pm, \mp) parity results for the qubits associated with the temporal and spatial modes $m q$ at the two sites. and the resulting memory state is

$$\begin{aligned} |\chi_{\overline{AB}, m}^{(s)}(\mathbf{h})\rangle &= \frac{1}{\sqrt{2}} \sum_{q=0}^{K-1} \eta_q(x_s) \left(e^{i\beta x_s} |0_{\overline{A}}, 1_{\overline{B} m q}\rangle \right. \\ &\quad \left. + f(\mathbf{h}_{m q}) e^{-i\beta x_s} |1_{\overline{A} m q}, 0_{\overline{B}}\rangle \right). \end{aligned} \quad (47)$$

Here the conditional sign is given by

$$f(\mathbf{h}_{m q}) = \begin{cases} +1 & \text{for } h_{A m q} = \pm \text{ and } h_{B m q} = \pm \\ -1 & \text{for } h_{A m q} = \pm \text{ and } h_{B m q} = \mp \end{cases}, \quad (48)$$

where $h_{A m q}$ and $h_{B m q}$ are the results of the X basis measurements of the photonic qubits corresponding to the time bin m and spatial mode q at the two sites. We should mention that at this point, we do not yet know the temporal and spatial mode $m q$ of the incoming photon, and therefore cannot tell if $f(\mathbf{h}_{m q})$ is 1 or -1 . Thus at this stage, we have to simply store the results of all the X basis measurement results in a classical memory register for now. Once we go through the decoding stage and determine the temporal and spatial mode, then we will be able to look at these stored results and see if $f(\mathbf{h}_{m q})$ is 1 or -1 , depending on whether the corresponding photonic qubit results have even or odd parity, respectively. Therefore, $h_{A m q}$ and $h_{B m q}$ are entries of a $2KM$ -component array h containing the results of all the X basis measurement outcomes.

The density matrix for the memory system is then

$$\begin{aligned} \sigma_{\overline{AB}}(\mathbf{h}) &= (1 - M\epsilon)\sigma_{\overline{AB}, 0} \\ &\quad + \frac{\epsilon}{2} \sum_{\substack{m=1 \\ s \in \{1, 2\}}}^M |\chi_{\overline{AB}, m}^{(s)}(\mathbf{h})\rangle \langle \chi_{\overline{AB}, m}^{(s)}(\mathbf{h})|. \end{aligned} \quad (49)$$

The encoding of the arrival time is complete, nonetheless, we require the collapse of the superposition over index q via a projective measurement, which is accomplished in the decoding step which we describe in the next section. The implementation of the encoding would require the interaction of the incoming photon with an atomic cavity, similar to the one described in Ref. [54]. As for the measurement of the photonic state in the X basis, it has been suggested in Ref. [41] that it could be approximated by mixing the photon with ancillary states in an interferometer, and in principle, the larger the interferometer, the closer we could be to a deterministic X -basis measurement. A more careful study of this proposal and an alternative method for a deterministic X basis measurement will be presented in a future publication.

V. DECODING

We now proceed with the decoding step where we reveal the time bins in which the photons arrive. The employed tool is an ancilla consisting of $K\overline{M}$ entangled pairs described by the sets of systems C and D . This ancilla state has the form

$$|\Phi_{CD}\rangle = \bigotimes_{i=0}^{K-1} \bigotimes_{k=1}^{\overline{M}} |\phi_{C_{ki} D_{ki}}^+\rangle. \quad (50)$$

where $|\phi_{C_{ki} D_{ki}}^+\rangle = (|0_{C_{ki}}, 0_{D_{ki}}\rangle + |1_{C_{ki}}, 1_{D_{ki}}\rangle)/\sqrt{2}$. We will then employ a circuit that flip some or all of these into $|\phi_{C_{ki} D_{ki}}^-\rangle = (|0_{C_{ki}}, 0_{D_{ki}}\rangle - |1_{C_{ki}}, 1_{D_{ki}}\rangle)/\sqrt{2}$, if some of the memory qubits are in $|1\rangle$ due to an incoming photon in the original photonic system. The Bell states upon measurement in the X basis, will yield ‘even’ or ‘odd’ parity results and reveal which of the Bell states underwent a flip and allow us to determine the spatio-temporal mode of the incoming photon, as we will shortly describe. This step is also known as ‘checking’ the parity.

Systems C_{ki} and D_{ki} are sent to sites A and B , respectively. The decoding step involves the application of Controlled Z (CZ) gates where the state of the memory acts as the control qubit whereas the target qubit comes from the pre-shared entangled ancilla (note that all the $|\phi_{C_{ki} D_{ki}}^{\pm}\rangle$ pairs are identical and the index is used to keep track of which Bell pair is acted on by the CZ gates). The mapping is carried out with the operator defined as

$$V \equiv \bigotimes_{i=0}^{K-1} \bigotimes_{k=1}^{\overline{M}} \left(V_{\overline{A}_{ki} C_{ki}} \otimes V_{\overline{B}_{ki} D_{ki}} \right), \quad (51)$$

where the indices $(\overline{A}_{ki}, \overline{B}_{ki})$ and (C_{ki}, D_{ki}) represent the control and target qubits, respectively. The effects of these gates are

$$\begin{aligned} V_{\overline{A}_{ki}, C_{ki}} V_{\overline{B}_{ki}, D_{ki}} |0_{\overline{A}_{ki}}, 1_{\overline{B}_{ki}}\rangle |\phi_{C_{ki} D_{ki}}^+\rangle \\ = |0_{\overline{A}_{ki}}, 1_{\overline{B}_{ki}}\rangle |\phi_{C_{ki} D_{ki}}^-\rangle, \end{aligned} \quad (52a)$$

$$\begin{aligned} V_{\overline{A}_{ki}, C_{ki}} V_{\overline{B}_{ki}, D_{ki}} |1_{\overline{A}_{ki}}, 0_{\overline{B}_{ki}}\rangle |\phi_{C_{ki} D_{ki}}^+\rangle \\ = |1_{\overline{A}_{ki}}, 0_{\overline{B}_{ki}}\rangle |\phi_{C_{ki} D_{ki}}^-\rangle, \end{aligned} \quad (52b)$$

$$\begin{aligned} V_{\overline{A}_{ki}, C_{ki}} V_{\overline{B}_{ki}, D_{ki}} |0_{\overline{A}_{ki}}, 0_{\overline{B}_{ki}}\rangle |\phi_{C_{ki} D_{ki}}^+\rangle \\ = |0_{\overline{A}_{ki}}, 0_{\overline{B}_{ki}}\rangle |\phi_{C_{ki} D_{ki}}^+\rangle, \end{aligned} \quad (52c)$$

$$\begin{aligned} V_{\overline{A}_{ki}, C_{ki}} V_{\overline{B}_{ki}, D_{ki}} |1_{\overline{A}_{ki}}, 1_{\overline{B}_{ki}}\rangle |\phi_{C_{ki} D_{ki}}^+\rangle \\ = |1_{\overline{A}_{ki}}, 1_{\overline{B}_{ki}}\rangle |\phi_{C_{ki} D_{ki}}^+\rangle, \end{aligned} \quad (52d)$$

i.e., for odd memory pairs, $|\phi_{C_{ki} D_{ki}}^+\rangle$ transforms into $|\phi_{C_{ki} D_{ki}}^-\rangle = (|0_{C_{ki}}, 0_{D_{ki}}\rangle - |1_{C_{ki}}, 1_{D_{ki}}\rangle)/\sqrt{2}$, and even pairs leave the state $|\phi_{C_{ki} D_{ki}}^+\rangle$ unchanged. Thus with the application of the CZ operations from the memory state (47) to systems C and D , we obtain

$$\left| \chi_{\overline{ABCD},m}^{(s)}(\mathbf{h}) \right\rangle = V \left| \chi_{\overline{AB},m}^{(s)}(\mathbf{h}) \right\rangle |\Phi_{CD}\rangle \quad (53a)$$

$$= V \frac{1}{\sqrt{2}} \sum_{q=0}^{K-1} \eta_q(x_s) \left(e^{i\beta x_s} \left| 0_{\overline{A}}, 1_{\overline{B}mq} \right\rangle + f(\mathbf{h}_{mq}) e^{-i\beta x_s} \left| 1_{\overline{A}mq}, 0_{\overline{B}} \right\rangle \right) \bigotimes_{i=0}^{K-1} \bigotimes_{k=1}^{\overline{M}} \left| \phi_{C_{ki}D_{ki}}^+ \right\rangle \quad (53b)$$

$$= \sum_{q=0}^{K-1} \eta_q(x_s) \left| \chi_{\overline{AB},mq}^{(s)}(\mathbf{h}) \right\rangle |\Phi_{CD,mq}\rangle, \quad (53c)$$

where

$$\left| \chi_{\overline{AB},mq}^{(s)}(\mathbf{h}) \right\rangle = \frac{1}{\sqrt{2}} \left(e^{i\beta x_s} \left| 0_{\overline{A}}, 1_{\overline{B}mq} \right\rangle + f(\mathbf{h}_{mq}) e^{-i\beta x_s} \left| 1_{\overline{A}mq}, 0_{\overline{B}} \right\rangle \right) \quad (54)$$

is the superposition of memories corresponding to an excitation in modes q and m , and

$$\begin{aligned} |\Phi_{CD,mq}\rangle &= \bigotimes_{i=0}^{K-1} \bigotimes_{k=1}^{\overline{M}} (Z_{C_{ki}})^{\delta_{iq} w_{km}} \left| \phi_{C_{ki}D_{ki}}^+ \right\rangle \\ &= \bigotimes_{i=0}^{K-1} \bigotimes_{k=1}^{\overline{M}} (Z_{D_{ki}})^{\delta_{iq} w_{km}} \left| \phi_{C_{ki}D_{ki}}^+ \right\rangle \end{aligned} \quad (55)$$

is the Bell state ancilla after the unitary V has been applied. The Pauli operators $Z_{C_{ki}}$ and $Z_{D_{ki}}$ have the effect of flipping the sign of the relevant Bell pairs according to the rules (52a)-(52d) (by acting on qubit ki of system C and D), respectively. The power δ_{iq} means that this operator is acting only when $i = q$, and w_{km} means it is happening only for the Bell pairs corresponding to the binary representation of the temporal mode number m . In short, if we have an incoming photon in temporal mode m , then in each term of our state, the Bell pairs corresponding to the spatio-temporal mode mq undergo a flip, while the remaining Bell states are unflipped. On the other hand, the action of V on the first term of (49) associated with the photonic vacuum of systems A and B , will leave all the Bell pairs unaffected: $V|0_{\overline{A}}, 0_{\overline{B}}\rangle|\Phi_{CD}\rangle = |0_{\overline{A}}, 0_{\overline{B}}\rangle|\Phi_{CD}\rangle$.

Before performing the parity checks, we write the Bell states in terms of the X basis:

$$\left| \phi_{C_{ki}D_{ki}}^+ \right\rangle = \frac{1}{\sqrt{2}} (|+_{C_{ki}}, +_{D_{ki}}\rangle + |-_{C_{ki}}, -_{D_{ki}}\rangle) \quad (56)$$

and

$$\left| \phi_{C_{ki}D_{ki}}^- \right\rangle = \frac{1}{\sqrt{2}} (|+_{C_{ki}}, -_{D_{ki}}\rangle + |-_{C_{ki}}, +_{D_{ki}}\rangle). \quad (57)$$

This means that if we perform X basis measurements on all the qubits of the ancilla Bell states, we will obtain even parity results $|+_{C_{ki}+D_{ki}}\rangle$ or $|-_{C_{ki}-D_{ki}}\rangle$ for all the unflipped Bell pairs and odd parity results $|+_{C_{ki}-D_{ki}}\rangle$ or $|-_{C_{ki}+D_{ki}}\rangle$ for the Bell pairs flipped by the CZ operations. This way, an X basis measurement will tell us which memory qubits have the excitations. It will reveal the time bin in which the photon arrived, and also serve as a projective measurement for determining its spatial mode. This will collapse the sum over the spatial modes in state (53c), giving us the resulting state of the memory qubits

$$\sigma_{\overline{AB},mq}(\mathbf{h}) = \frac{1}{2} \sum_{s \in \{1,2\}} \left| \chi_{\overline{AB},mq}^{(s)}(\mathbf{h}) \right\rangle \left\langle \chi_{\overline{AB},mq}^{(s)}(\mathbf{h}) \right| \quad (58)$$

with corresponding probabilities (conditional upon there being an incoming photon)

$$p_q(\theta) = \eta_q^2(\theta). \quad (59)$$

Having found the spatial mode, the remaining task is to determine if the photon is in the symmetric or anti-symmetric combination of mode q collected at the two sites. Now, the memory qubits corresponding to the unflipped Bell states Now, the memory qubits corresponding to the unflipped Bell states (i.e. the ones found to have even parity) are all in $|0\rangle$. These contain no useful information and we can drop them going forward. This leaves only the memory qubits corresponding to the Bell pairs found to be in $|\phi^-\rangle$ (i.e. the ones for which we obtained odd parity results). Let $N_m \in \{1, \dots, \overline{M}\}$ be the number of such Bell pairs found to have flipped into $|\phi^-\rangle$ after the CZ gates step for a given time bin m in which the photon arrived. We can now define subsystems E and F containing only the $2N_m$ remaining memory qubits, and we adopt the labeling $\gamma \in \{E, F\}$ for these new systems. Then we construct the reduced state consisting of $2N_m$ entangled qubits, and this has the form

$$\nu_{EF,mq}(\mathbf{h}) = \frac{1}{2} \sum_{s \in \{1,2\}} \left| \omega_{EF,mq}^{(s)}(\mathbf{h}) \right\rangle \left\langle \omega_{EF,mq}^{(s)}(\mathbf{h}) \right|, \quad (60)$$

where

$$\begin{aligned} \left| \omega_{EF,mq}^{(s)}(\mathbf{h}) \right\rangle &= \frac{1}{\sqrt{2}} \left(e^{i\beta x_s} \left| \mathbf{0}_{Emq}, \mathbf{1}_{Fmq} \right\rangle \right. \\ &\quad \left. + f(\mathbf{h}_{mq}) e^{-i\beta x_s} \left| \mathbf{1}_{Emq}, \mathbf{0}_{Fmq} \right\rangle \right), \end{aligned} \quad (61)$$

with new kets defined as

$$\left| \mathbf{0}_{Emq}, \mathbf{1}_{Fmq} \right\rangle = \bigotimes_{\mu=1}^{N_m} \left| 0_{E\mu q}, 1_{F\mu q} \right\rangle \quad (62)$$

and

$$\left| \mathbf{1}_{Emq}, \mathbf{0}_{Fmq} \right\rangle = \bigotimes_{\mu=1}^{N_m} \left| 1_{E\mu q}, 0_{F\mu q} \right\rangle. \quad (63)$$

Note that we have defined the states (61) in terms of x_s . We will make the substitutions $x_1 = \theta$ and $x_2 = -\theta$ for our 2-point problem later.

To determine if the incoming photon was in the symmetric or anti-symmetric combination of the q mode signals collected at the two sites, we need to measure this in the basis

$$\left| \zeta_{EF,mq}^\pm \right\rangle = \frac{1}{\sqrt{2}} (|\mathbf{0}_{Emq}, \mathbf{1}_{Fmq}\rangle \pm |\mathbf{1}_{Emq}, \mathbf{0}_{Fmq}\rangle), \quad (64)$$

The measurement interpretations will depend on the value of $f(\mathbf{h}_{mq})$ which we know from the X basis measurement outcomes of the photonic qubit measurements described in the encoding section. Since the parity checks of the Bell pairs have by now revealed the temporal mode m of the incoming photon and collapsed the state to a particular spatial mode q , we now revert to our stored results for our X basis measurement of the corresponding photonic qubits at the end of the encoding section. To remind the reader, we obtain $f(\mathbf{h}_{mq}) = \pm 1$ for even/odd parity results, respectively.

Now, when $f(\mathbf{h}_{mq}) = 1$, measuring in the $|\zeta_{\pm}\rangle$ states corresponds to measuring in the basis $|\phi_{AB,q}^{\pm}\rangle$, stated in equations (23). Whereas when $f(\mathbf{h}_{mq}) = -1$, then these flip due to the minus sign, so the $|\zeta_{EF,mq}^{\pm}\rangle$ measurement corresponds to measuring in $|\phi_{AB,q}^{\mp}\rangle$.

To obtain the measurement probabilities, we write (61) in terms of $|\zeta_{EF,mq}^{\pm}\rangle$, obtaining

$$\begin{aligned} |\omega_{EF,mq}^{(s)}(\mathbf{h})\rangle &= \frac{1}{2} \left(e^{i\beta x_s} + f(\mathbf{h}_{mq})e^{-i\beta x_s} \right) |\zeta_{EF,mq}^+\rangle \\ &\quad + \frac{1}{2} \left(e^{i\beta x_s} - f(\mathbf{h}_{mq})e^{-i\beta x_s} \right) |\zeta_{EF,mq}^-\rangle \\ &= c_+^{(s)}(\mathbf{h}_{mq}) |\zeta_{EF,mq}^+\rangle + c_-^{(s)}(\mathbf{h}_{mq}) |\zeta_{EF,mq}^-\rangle, \end{aligned} \quad (65a)$$

where

$$c_{\pm}^{(s)}(\mathbf{h}_{mq}) \equiv \frac{1}{2} \left(e^{i\beta x_s} \pm f(\mathbf{h}_{mq})e^{-i\beta x_s} \right) \quad (66)$$

are the probability amplitudes of obtaining the measurement outcome $|\zeta_{EF,mq}^+\rangle$ or $|\zeta_{EF,mq}^-\rangle$, respectively.

At this point, the task of measuring (61) in the (64) states is, in principle, a GHZ state measurement. This can be done by measuring each qubit in the X -basis and then considering the parities of the outcomes associated with the results for each pair of qubits at both sites corresponding to the same digit of the binary encoding of the spatio-temporal mode mq . We show in appendix B that an even number of odd parity results i.e. $|+_{E\mu q}, -_{F\mu q}\rangle$ or $|-_{E\mu q}, +_{F\mu q}\rangle$ means finding the state to be $|\zeta_{mq}^+\rangle$, and an odd number of odd parity results signifies obtaining $|\zeta_{EF,mq}^-\rangle$ as our measurement outcome. Putting together the pieces along with the two cases for $f(\mathbf{h}_{mq})$, we obtain the conditional probabilities $p_{\pm}(x_s)$ that given an incoming photon is in spatial mode q , it is in the symmetric or anti-symmetric combinations $|\phi_{AB,q}^{\pm}\rangle$ of the signals collected at the two sites

$$p_+(x_s) = [c_+^{(s)}(\mathbf{h})]^2 = \cos^2(\beta x_s) \quad (67)$$

$$p_-(x_s) = [c_+^{(s)}(\mathbf{h})]^2 = \sin^2(\beta x_s) \quad (68)$$

for $f(\mathbf{h}_{mq}) = 1$, and

$$p_+(x_s) = [c_-^{(s)}(\mathbf{h})]^2 = \cos^2(\beta x_s) \quad (69)$$

$$p_-(x_s) = [c_-^{(s)}(\mathbf{h})]^2 = \sin^2(\beta x_s). \quad (70)$$

For $f(\mathbf{h}_{mq}) = -1$.

Overall, we obtain the full probabilities for a photon originating from a source at x_s to be in the modes $|\phi_{AB,q}^{\pm}\rangle$:

$$\begin{aligned} P_{q+}(x_s) &= p_+(x_s)P_q(x_s) = \cos^2(\beta x_s)\eta_q^2(x_s) \\ P_{q-}(x_s) &= p_-(x_s)P_q(x_s) = \sin^2(\beta x_s)\eta_q^2(x_s). \end{aligned} \quad (71)$$

The full probability of the symmetric and anti-symmetric states from both stars will be their brightness-weighted sum. Recalling that $x_1 = \theta$ and $x_2 = -\theta$, we obtain $P_{q\pm}(x_1) = P_{q\pm}(x_2) = P_{q\pm}(\theta)$ since $\eta_q^2(\theta)\cos^2(\beta\theta) = \eta_q^2(-\theta)\cos^2(-\beta\theta)$ and $\eta_q^2(\theta)\sin^2(\beta\theta) = \eta_q^2(-\theta)\sin^2(-\beta\theta)$. The total probability for a photon from either of the two stars to be in modes (23) will therefore be

$$P_{q\pm}(\theta) = \frac{1}{2} \sum_{s \in \{1,2\}} P_{q\pm}(x_s) = \frac{1}{2} [P_{q\pm}(\theta) + P_{q\pm}(-\theta)] \quad (72)$$

That is,

$$P_{q+}(\theta) = \eta_q^2(\theta)\cos^2(\beta\theta) \quad (73)$$

and

$$P_{q-}(\theta) = \eta_q^2(\theta)\sin^2(\beta\theta), \quad (74)$$

which are exactly the probabilities (24) and (25). These are exactly the probabilities from [29], except of course for the change that we are obtaining $\eta_q(\theta)$ in place of $\Gamma_q(\theta)$ due to the fact that we are only collecting the first K modes. As we mentioned earlier when we introduced $\eta_q(\theta)$ in (21), $\eta_q(\theta) \rightarrow \Gamma_q(\theta)$ when K is sufficiently large. We have thus reproduced the probabilities of the different measurement outcomes from [29] with our entanglement-based protocol as we set out to do.

VI. QUANTUM LIMIT OF PRECISION FOR ESTIMATING TWO-SOURCE SEPARATION

The maximum amount of physically allowed information we can obtain about an unknown parameter is given by the quantum Fisher information (QFI) [51]. For the two-source separation problem, Tsang *et al.* in [2] derive a general expression for the QFI matrix. For our convention of the stars positioned at $\pm\theta$, the component associated with the separation is

$$\mathcal{K} = 4N \int dx \left| \frac{\partial \psi(x)}{\partial x} \right|^2. \quad (75)$$

where $\psi(x)$ is the PSF, and N is the total number of incoming photons during the integration time. Taking the combined PSF (13) for our system system of 2 hard apertures, and setting $\beta = \pi r/\sigma$, where $r = 2\beta/\delta$ is the ratio between the mid-point separation 2β (between the two apertures) and the individual aperture size $\delta = 2\pi/\sigma$, gives the following QFI

$$\mathcal{K} = \frac{4\pi^2 N}{3\sigma^2} (3r^2 + 1). \quad (76)$$

This result was originally obtained in [29]. (Do note that in their conventions, the two apertures are at $\pm\beta/2$ instead of $\pm\beta$, hence their $r = \beta/\delta$, whereas we have $r = 2\beta/\delta$ in order to have the physically same r as them with the same QFI and CFI expressions.)

The performance of a particular measurement for determining an unknown parameter is given by the classical Fisher information (CFI). For a single parameter problem, the CFI for a discrete random variable is given by

$$\mathcal{J}(\theta) = N \sum_i \frac{1}{P_i} \left(\frac{\partial P_i}{\partial \theta} \right)^2, \quad (77)$$

where P_i is the probability of getting outcome i and N the number of copies of the state being measured. In our problem, the CFI for outcome probabilities (73) and (74) is

$$\mathcal{J}_q(\theta) = \frac{N_K}{P_{q+}(\theta)} \left(\frac{\partial P_{q+}(\theta)}{\partial \theta} \right)^2 + \frac{N_K}{P_{q-}(\theta)} \left(\frac{\partial P_{q-}(\theta)}{\partial \theta} \right)^2 \quad (78a)$$

$$= 4N_K \left[\beta^2 \eta_q^2(\theta) + [\eta'_q(\theta)]^2 \right], \quad (78b)$$

where as per (21), $\eta_q(\theta) \equiv \Gamma_q(\theta) / \sqrt{\sum_{i=0}^{K-1} \Gamma_i^2(\theta)}$ and $\eta'_q(\theta) = \partial \eta_q(\theta) / \partial \theta$. N_K is the (average) number of incoming photons in the first K spatial modes and is given by (22).

We can now add the CFI contributions over all the spatial modes

$$\mathcal{J}_{K\text{-SPADE}}(\theta) = \sum_{q=0}^{K-1} \mathcal{J}_q(\theta) \quad (79a)$$

$$= 4N_K \left[\frac{\pi^2 r^2}{\sigma^2} + \sum_{q=0}^{K-1} [\eta'_q(\theta)]^2 \right] \quad (79b)$$

$$= 4N \left\{ \left[\sum_{q=0}^{K-1} \frac{\pi^2 r^2}{\sigma^2} \Gamma_q^2(\theta) + [\Gamma'_q(\theta)]^2 \right] - \frac{\left(\sum_{i=0}^{K-1} \Gamma_i(\theta) \Gamma'_i(\theta) \right)^2}{\sum_{j=0}^{K-1} \Gamma_j^2(\theta)} \right\}, \quad (79c)$$

where in the second step, we have used $\sum_{q=0}^{K-1} \eta_q^2(\theta) = 1$ from the normalization condition and $\beta = \pi r / \sigma$. In the last step, we have used (22) and (21) to express the result in terms of the total incoming photon flux N (in all the spatial modes) and the single-aperture correlation functions $\Gamma_q(\theta)$ and their derivatives. In the large K limit, $\sum_{q=0}^{K-1} \Gamma_q(\theta) \rightarrow 1$ from normalization. Then for our special case of a hard aperture with a sinc function PSF (10), and taking the mode functions to be the normalized sinc-bessel modes $\phi_q(\theta)$, we find that when $K \rightarrow \infty$, the total CFI approaches the QFI [29]

$$\lim_{K \rightarrow \infty} \mathcal{J}_{K\text{-SPADE}}(\theta) = \frac{4\pi^2 N}{3\sigma^2} (3r^2 + 1) = \mathcal{K}, \quad (80)$$

In Fig. 3, the CFI is plotted normalized with respect to the QFI for different values of K and r . One can see how increasing these two parameters the CFI approaches the QFI in the small θ/σ limit.

Note in the QFI (and CFI for the $K \rightarrow \infty$ case) that $4N\pi^2/3\sigma^2$ is in fact equal to the QFI for just a single aperture [3, 29, 55]. So having two apertures is resulting in a gain by a factor of $3r^2 + 1$. The $3r^2$ term thus contains the extra information arising from having two apertures and employing baseline interferometry, whereas the other piece is just the single-aperture QFI. In the above expressions, it is straightforward to see that resolving the light collected by the two apertures into spatial modes contributes to the latter piece whereas the former is obtained by combining the signals from the two telescopes [29].

While we have derived the QFI and CFI result for the one-dimensional version of the problem, it turns out that this has a rather nice interpretation for the two-dimensional case. Let us assume that our two apertures are still located at positions $\pm\beta$ along the horizontal axis of the aperture plane, but each

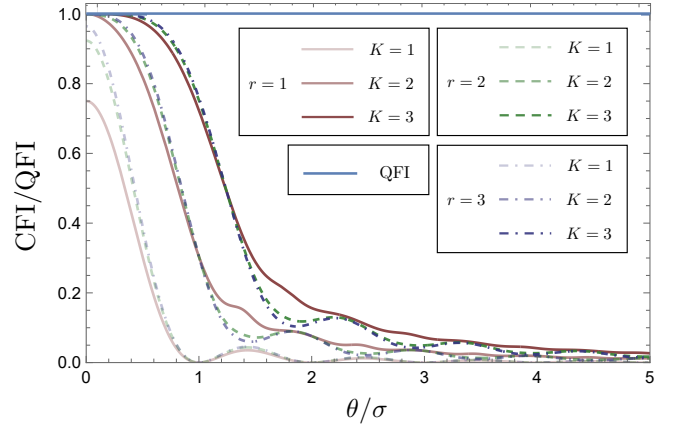


FIG. 3. Plots of the normalized CFI with respect to the QFI for three different ratios: $r = 1$ (solid lines), $r = 2$ (dashed lines) and $r = 3$ (dot-dashed lines).

of these is now a square of length δ instead of being a one-dimensional rect function. The 2-dimensional equally bright two-point separation estimation problem has been worked out in [5], where they calculate the QFI matrix in cartesian coordinates for the x and y components of the separation with a single aperture. Combining that with the multiple-aperture framework introduced in [29], we can calculate the QFI for the x -component of the separation. We outline this calculation in appendix C. Moreover, we can follow the same protocol described above in order to measure the incoming photons in the pairwise combinations of the (2-dimensional) local modes of the two apertures, and in the large K limit, it will again attain the QFI which will be given by the same expression $4N\pi^2(3r^2 + 1)/\sigma^2$ [56].

Now, recall that $\sigma = 2\pi/\delta$, with δ the size and $r = 2\beta/\delta$. Also, the total number N of photons collected during the integration time will be proportional to the area of the apertures δ^2 . So all in all, the $4N\pi^2/\sigma^2$ factor will scale as δ^4 . The $3r^2$ term in the QFI will scale as $\delta^2\beta^2$, whereas the other term will be proportional to δ^4 . This tells us that as δ gets larger (or equivalently as r is small and closer to unity), we will get more information from the spatial mode resolution of the light within each aperture.

VII. GENERALIZATION TO MULTIPLE TELESCOPES AND MORE COMPLEX IMAGING PROBLEMS

Since the QFI-attaining measurement for any single-parameter estimation task—no matter how complex the scene and its configuration—is a von Neumann projective measurement, given the one-photon-per-temporal-conherence-interval assumption, the QFI attaining measurement can always be expressed as a linear interferometric unitary transformation among all the locally-collected spatial modes across all the telescopes in the baseline, followed by shot-noise-limited photon detection on the output modes. We now discuss how the protocol we present in this paper can be generalized to measuring the incoming photons in such an arbitrary linear combination basis of the local modes collected by any number

of telescopes. Say we have n telescopes and we are collecting K mutually-orthogonal spatial modes at each site. And our goal is to measure the photons in some arbitrary set of mutually orthogonal linear combinations of these nK signals. If we are carrying out such a measurement by bringing all the nK mode signals to a central location through single mode fibers, then we can use a beam splitter circuit to create an interferometer that mixes all the signals in the desired set of linear combinations. It has been shown in [38] that we can create such an interferometer that gives us any desired unitary transformation between the nK inputs and the same number of outputs by employing $nK(nK - 1)/2$ Mach Zehnder interferometers (MZIs). Since an MZI comprises of two 50-50 beam splitters and two tunable phase shifts, this means a total of $nK(nK - 1)$ 50-50 beam splitters and the same number of phase shifts is needed. If we are using pre-shared entanglement to accomplish this losslessly, instead of using (lossy) single mode fibers and beam splitters, then we need three ingredients:

1. An entanglement based protocol that mimics a fifty-fifty beam splitter between two modes whose quantum state resides in the span of one photon spread across the two modes, at two distant sites. We will shortly make this statement more precise and show that we can indeed accomplish this.
2. The ability to apply any arbitrary phase shift to an optical mode, or a single-qubit phase after the light-to-qubit transduction explained in the paper. This can be accomplished easily in either domain.
3. (Optional) An n site generalization of our procedure of using Bell states ancillas to determine the spatio-temporal mode of an incoming photon, to possibly realize the nonlocal version of the Clements *et al.* circuit [38] more resource-efficiently. It is straightforward to see that this can be accomplished by employing a GHZ state in place of a Bell state (to realize a three-qubit nonlocal Clifford unitary) and using CZ gates just as we did in Section V.

We now show how to mimic a fifty-fifty beam splitter on the space limited to zero or one photon among two modes. Consider the input modes A and B of a 50-50 beam splitter with outputs A' and B' . The beam splitter will have the action:

$$a|1_A 0_B\rangle + b|0_A 1_B\rangle \quad (81)$$

$$\downarrow$$

$$\frac{a+b}{\sqrt{2}}|1_{A'} 0_{B'}\rangle + \frac{a-b}{\sqrt{2}}|0_{A'} 1_{B'}\rangle \quad (82)$$

$$\downarrow$$

$$|0_A 0_B\rangle \quad (83)$$

$$\downarrow$$

$$|0_{A'} 0_{B'}\rangle. \quad (84)$$

Interpreting the above states of two modes as states of two *single-rail* qubits (i.e., qubits encoded by the absence or the presence of a single photon in a mode), it is easy to see that the above can be accomplished by carrying out the following sequence of operations:

1. A CNOT gate from qubit A to B .
2. The Hadamard gate on qubit A .

3. A CNOT gate from qubit A to B .

With the two qubits at two different sites, the CNOT operations need to be carried out through gate teleportation, which consumes one pre-shared two-qubit Bell state, each, in a way identical to that in Ref. [57]. We have thus shown how to mimic a 50-50 beam splitter across two sites. We can therefore use this and apply the framework in [38] to mimic any nonlocal multimode beam splitter circuit to measure the incoming photons in any arbitrary collective basis.

VIII. CONCLUSION

Shared entanglement offers a very interesting and potentially promising direction for long-baseline interferometry over large distances that are currently not feasible with traditional techniques due to losses and other practical constraints. However, this still remains a largely unexplored direction with a few pioneering works such as [34] and [35] proposing how to estimate the phase difference between two sites using shared entanglement, which amounts to estimating the location of a single monochromatic point source. The former work introduces this concept and the latter provides a way to do this with substantially fewer entanglement resources with a logarithmic compression of the information-bearing light into atomic qubit registers. Here we have taken a step towards combining these ideas with a suite of recent research on pre-detection spatial mode sorting to achieve quantum-limited spatial resolution of a single telescope, to addressing general quantitative imaging and parameter estimation tasks with long-baseline telescope arrays. Our approach involves sorting the light collected at each telescope site into a few highest-order local spatial modes, storing the information bearing light in each sorted mode into atomic qubit memory registers, and using shared entanglement among the telescope sites to effect the multimode linear optical mode mixing prior to detection, but without bringing the light from the telescopes to one common location. For the problem of estimating the separation between two point sources, leveraging the result from [29]—which proved that the QFI-attaining measurement involves measuring the incoming light in terms of the sums and differences of the modal signal amplitudes received at the two telescopes, we fully work out our qubit-efficient interferometric technique to realize this QFI-attaining measurement in a non-local fashion. We also outline how our protocol can be generalized to an entanglement based recipe to attain the quantum limit for any quantitative imaging or parameter estimation problem. We hope this will inspire more research towards eventually building a real long baseline interferometric system that employs high-fidelity shared entanglement, which brings together spatial-mode sorting, programmable linear optics, efficient light-matter interfaces to spin qubits, and high-fidelity quantum logic among spin qubits in one working system.

IX. ACKNOWLEDGEMENTS

The authors thank Michael Grace for helpful discussions, and Prajit Dhara for comments on the manuscript. This work was co-funded by AFOSR grant number FA9550-22-1-0180 and NASA grant number 80NSSC22K1030.

Appendix A: Derivation of the M -copy state of the incoming light state

Here we present a more detailed derivation of Eq. (28) from the main text. The key to understand these steps is that expand the state time bin at a time, so that in every step we get rid of all the non-linear terms of the mean photon number ϵ . For example, we can begin by computing the tensor product of two copies of ρ_{AB} :

$$\rho_{AB}^{\otimes 2} = [(1 - \epsilon)\rho_{0,AB} + \epsilon\rho_{1,AB}]^{\otimes 2} \quad (\text{A1a})$$

$$= (1 - \epsilon)^2 \rho_{0,AB}^{\otimes 2} + (1 - \epsilon)\epsilon(\rho_{0,AB} \otimes \rho_{1,AB} + \rho_{1,AB} \otimes \rho_{0,AB}) + \epsilon^2 \rho_{1,AB}^{\otimes 2} \quad (\text{A1b})$$

$$= (1 - 2\epsilon)\rho_{0,AB}^{\otimes 2} + \epsilon(\rho_{0,AB} \otimes \rho_{1,AB} + \rho_{1,AB} \otimes \rho_{0,AB}) + \epsilon^2(\rho_{0,AB}^{\otimes 2} - \rho_{0,AB} \otimes \rho_{1,AB} - \rho_{1,AB} \otimes \rho_{0,AB} + \rho_{1,AB}^{\otimes 2}). \quad (\text{A1c})$$

Since the non-linear terms of ϵ are neglected, we can drop the ϵ^2 term. Thus,

$$\rho_{AB}^{\otimes 2} \approx (1 - 2\epsilon)\rho_{0,AB}^{\otimes 2} + \epsilon(\rho_{0,AB} \otimes \rho_{1,AB} + \rho_{1,AB} \otimes \rho_{0,AB}). \quad (\text{A2})$$

Now we repeat this procedure over the M time bins:

$$\rho_{AB}^{\otimes M} = [(1 - \epsilon)\rho_{0,AB} + \epsilon\rho_{1,AB}]^{\otimes M} \quad (\text{A3a})$$

$$\approx [(1 - 2\epsilon)\rho_{0,AB}^{\otimes 2} + \epsilon(\rho_{0,AB} \otimes \rho_{1,AB} + \rho_{1,AB} \otimes \rho_{0,AB})] \otimes \rho_{0,AB}^{\otimes (M-2)} \quad (\text{A3b})$$

$$\approx [(1 - 3\epsilon)\rho_{0,AB}^{\otimes 3} + \epsilon(\rho_{1,AB} \otimes \rho_{0,AB} \otimes \rho_{0,AB} + \rho_{0,AB} \otimes \rho_{1,AB} \otimes \rho_{0,AB} + \rho_{0,AB} \otimes \rho_{0,AB} \otimes \rho_{1,AB})] \otimes \rho_{AB}^{\otimes (M-3)} \quad (\text{A3c})$$

\vdots

$$\approx (1 - M\epsilon)\rho_{0,AB}^{\otimes M} + \epsilon \sum_{m=1}^M \rho_{1,AB,m}, \quad (\text{A3d})$$

with

$$\rho_{1,AB,m} \equiv \rho_{0,AB}^{\otimes (m-1)} \otimes \rho_{1,AB} \otimes \rho_{0,AB}^{\otimes (M-m)} \quad (\text{A3e})$$

being defined to represent a one-photon state in the m -th time bin.

Appendix B: Measurement in the $|\zeta_{EF,mq}^{\pm}\rangle$ states

Here we show how we can measure the state (61) in the (64) basis. At each site, we have n_m qubits labeled by an index $\mu = 1 \dots n_m$. We measure each qubit in the X basis and for each μ , compare whether the results at both sites are the same (i.e. $++$ or $--$ which we call even parity outcomes) or opposite (i.e. $+-$ or $-+$ which we call odd parity results). We will show that an even number of odd parity outcomes means we have $|\zeta_{mq}^+\rangle$, and obtaining an odd number of odd parities means $|\zeta_{mq}^-\rangle$. Now, the state for a single qubit in the first term is

$$|0_{E\mu q}, 1_{F\mu q}\rangle = \frac{1}{2} [(|+_{E\mu q}, +_{F\mu q}\rangle - |-_{E\mu q}, -_{F\mu q}\rangle) + (|+_{E\mu q}, -_{F\mu q}\rangle - |-_{E\mu q}, +_{F\mu q}\rangle)] \quad (\text{B1})$$

$$= \frac{1}{\sqrt{2}} (|e_{EF,\mu q}\rangle + |o_{EF,\mu q}\rangle) \quad (\text{B2})$$

and in the second term, we have

$$|1_{E\mu q}, 0_{F\mu q}\rangle = \frac{1}{2} [(|+_{E\mu q}, +_{F\mu q}\rangle - |-_{E\mu q}, -_{F\mu q}\rangle) - (|+_{E\mu q}, -_{F\mu q}\rangle - |-_{E\mu q}, +_{F\mu q}\rangle)] \quad (\text{B3})$$

$$= \frac{1}{\sqrt{2}} (|e_{EF,\mu q}\rangle - |o_{EF,\mu q}\rangle) \quad (\text{B4})$$

where

$$|e_{EF,\mu q}\rangle = \frac{1}{\sqrt{2}} (|+_{E\mu q}, +_{F\mu q}\rangle + |-_{E\mu q}, -_{F\mu q}\rangle) \quad (\text{B5})$$

are the even parity states, and

$$|o_{EF,\mu q}\rangle = \frac{1}{\sqrt{2}} (|-_{E\mu q}, +_{F\mu q}\rangle - |+_{E\mu q}, -_{F\mu q}\rangle). \quad (\text{B6})$$

are the odd parity states. So the even parity state (B5) has the same sign in both $|0_{E_{\mu q}}, 1_{F_{\mu q}}\rangle$ and $|1_{E_{\mu q}}, 0_{F_{\mu q}}\rangle$, but the odd parity state (B6) has opposite signs.

Now we need to expand N_m copies of $|0_{E_{\mu q}}, 1_{F_{\mu q}}\rangle$, and N_m copies of $|1_{E_{\mu q}}, 0_{F_{\mu q}}\rangle$. In the former, i.e., $|0_{E_{\mu q}}, 1_{F_{\mu q}}\rangle^{\otimes N_m}$, all the terms will have positive signs since a single copy has positive signs in front of both $|e_{EF,\mu q}\rangle$ and $|o_{EF,\mu q}\rangle$. But in $|1_{E_{\mu q}}, 0_{F_{\mu q}}\rangle^{\otimes N_m}$, all terms with an odd number of $|o_{EF,\mu q}\rangle$ will have minus signs. In other words, terms with an even number of $|o_{EF,\mu q}\rangle$ will have positive signs and will contribute to $|\zeta_{mq}^+\rangle$, but terms having an odd number of $|o_{EF,\mu q}\rangle$ will have minus signs and will contribute to $|\zeta_{mq}^-\rangle$. We have thus shown that we can measure whether we have $|\zeta_{EF,mq}^+\rangle$ or $|\zeta_{EF,mq}^-\rangle$ depending on whether we have an even or odd number of odd parity results, respectively.

Appendix C: The 2-dimensional QFI

The two-dimensional version of the equally bright two-point separation estimation problem has been worked out in [5], where they calculate the QFI matrix for the x and y components of the centroid and separation. They find that if the (2-dimensional) PSF has reflection symmetry in both x and y directions i.e. $\psi_{2d}(x, y) = \psi_{2d}(-x, y) = \psi_{2d}(x, -y) = \psi_{2d}(-x, -y)$, then the off-diagonal entries of the QFI matrix vanish and we can estimate the x and y components of the separation independently. The QFI components are then given by

$$\begin{aligned}\mathcal{K}_x &= 4N \int dx dy (\partial_x \psi_{2d}(x, y))^2 \\ \mathcal{K}_y &= 4N \int dx dy (\partial_y \psi_{2d}(x, y))^2\end{aligned}\tag{C1}$$

For simplicity, if we assume a square shaped aperture of length δ , then our 2d PSF for a single aperture will simply be $\psi_{2d, 1ap}(x, y) = \psi(x)\psi(y)$, where $\psi(x)$ is the 1-dimensional single-aperture PSF and was given in (10). Now, if we consider two such apertures along the horizontal axis of our aperture plane at positions β and $-\beta$, then following (12), the combined PSF will be

$$\psi_{2d, 2-ap}(x) = \sqrt{2} \cos(\beta x) \psi_{2d, 1ap}(x, y)\tag{C2}$$

Inserting this in (C1), we obtain $4N\pi^2(3r^2 + 1)/\sigma^2$ for the QFI for the horizontal component of the separation, same as the 1-dimensional QFI.

-
- [1] F. R. S. Lord Rayleigh, *Philosophical Magazine Series 5* **8**, 261 (1879).
- [2] M. Tsang, R. Nair, and X.-M. Lu, *Phys. Rev. X* **6**, 031033 (2016).
- [3] R. Kerviche, S. Guha, and A. Ashok, in *2017 IEEE International Symposium on Information Theory (ISIT)* (2017) pp. 441–445.
- [4] J. Řeháček, M. Paúr, B. Stoklasa, L. Motka, Z. Hradil, and L. L. Sánchez-Soto, [arXiv:1607.05837 \[quant-th\]](https://arxiv.org/abs/1607.05837).
- [5] S. Z. Ang, R. Nair, and M. Tsang, *Phys. Rev. A* **95**, 063847 (2017).
- [6] M. Tsang, *New Journal of Physics* **19**, 023054 (2017).
- [7] M. Tsang, (2019), [arXiv:1906.02064](https://arxiv.org/abs/1906.02064).
- [8] Z. Yu and S. Prasad, *Phys. Rev. Lett.* **121**, 180504 (2018).
- [9] S. Prasad and Z. Yu, *Phys. Rev. A* **99**, 022116 (2019).
- [10] J. Řeháček, Z. Hradil, B. Stoklasa, M. Paúr, J. Grover, A. Krzic, and L. L. Sánchez-Soto, *Phys. Rev. A* **96**, 062107 (2017).
- [11] J. Řeháček, Z. Hradil, D. Koutný, J. Grover, A. Krzic, and L. L. Sánchez-Soto, *Phys. Rev. A* **98**, 012103 (2018).
- [12] S. Prasad, *Physica Scripta* **95**, 054004 (2020).
- [13] E. Bisketzi, D. Branford, and A. Datta, *New Journal of Physics* **21**, 123032 (2019).
- [14] Z. Dutton, R. Kerviche, A. Ashok, and S. Guha, *Phys. Rev. A* **99**, 033847 (2019).
- [15] S. Prasad, *Phys. Rev. A* **102**, 063719 (2020).
- [16] M. Tsang, *Contemporary Physics* **60**, 279 (2019).
- [17] S. Zhou and L. Jiang, *Physical Review A* **99**, 013808 (2019).
- [18] X. M. Lu, H. Krovi, R. Nair, S. Guha, and J. H. Shapiro, *npj Quantum Information* **64** (2018).
- [19] Z. Huang and C. Lupo, *Physical Review Letters* **127**, 130502 (2021).
- [20] M. R. Grace and S. Guha, *Physical Review Letters* **129**, 180502 (2022).
- [21] F. Bao, H. Choi, V. Aggarwal, and Z. Jacob, *Opt. Lett.* **46**, 3045 (2021).
- [22] E. F. Matlin and L. J. Zipp, *Scientific Reports* **12** (2022), 10.1038/s41598-022-06644-3.
- [23] K. K. Lee, C. N. Gagatsos, S. Guha, and A. Ashok, *IEEE Journal of Selected Topics in Signal Processing*, **1** (2022).
- [24] A. Sajjad, M. R. Grace, Q. Zhuang, and S. Guha, *Phys. Rev. A* **104**, 022410 (2021).
- [25] M. R. Grace, Z. Dutton, A. Ashok, and S. Guha, *Journal of the Optical Society of America A* **37**, 1288 (2020).
- [26] C. Lupo, Z. Huang, and P. Kok, *Phys. Rev. Lett.* **124**, 080503 (2020).
- [27] Y. Wang, Y. Zhang, and V. O. Lorenz, *Physical Review A* **104**, 1 (2021).
- [28] M. Bojer, Z. Huang, S. Karl, S. Richter, P. Kok, and J. von Zanthier, *New Journal of Physics* **24**, 043026

- (2022).
- [29] A. Sajjad, M. R. Grace, and S. Guha, *Phys. Rev. Res.* **6**, 013212 (2024).
- [30] J. Campbell, in *Applied Geodesy*, edited by S. Turner (Springer Berlin Heidelberg, Berlin, Heidelberg, 1987) pp. 67–87.
- [31] *Principles of Long Baseline Stellar Interferometry* (2000).
- [32] J. D. Monnier, *Reports on Progress in Physics* **66**, 789 (2003).
- [33] Y. Huang, F. Salces-Carcoba, R. X. Adhikari, A. H. Safavi-Naeini, and L. Jiang, (2023), [arXiv:2312.09372](https://arxiv.org/abs/2312.09372) [quant-ph].
- [34] D. Gottesman, T. Jennewein, and S. Croke, *Phys. Rev. Lett.* **109**, 070503 (2012).
- [35] E. T. Khabiboulline, J. Borregaard, K. De Greve, and M. D. Lukin, *Phys. Rev. Lett.* **123**, 070504 (2019).
- [36] M. Tsang, R. Nair, and X.-M. Lu, (2016), [arXiv:1602.04655](https://arxiv.org/abs/1602.04655).
- [37] M. R. Grace and S. Guha, *Phys. Rev. Lett.* **129**, 180502 (2022).
- [38] W. R. Clements, P. C. Humphreys, B. J. Metcalf, W. S. Kolthammer, and I. A. Walmsley, *Optica* **3**, 1460 (2016).
- [39] K. S. Chou, J. Z. Blumoff, C. S. Wang, P. C. Reinhold, C. J. Axline, Y. Y. Gao, L. Frunzio, M. H. Devoret, L. Jiang, and R. J. Schoelkopf, *Nature* **561**, 368 (2018).
- [40] Z. S. Tang, K. Durak, and A. Ling, *Opt. Express* **24**, 22004 (2016).
- [41] E. T. Khabiboulline, J. Borregaard, K. De Greve, and M. D. Lukin, *Phys. Rev. A* **100**, 022316 (2019).
- [42] Z. Chen, A. Nomerotski, A. c. v. Slosar, P. Stankus, and S. Vintskevich, *Phys. Rev. D* **107**, 023015 (2023).
- [43] R. Czupryniak, J. Steinmetz, P. G. Kwiat, and A. N. Jordan, *Phys. Rev. A* **108**, 052408 (2023).
- [44] M. Pant, H. Krovi, D. Englund, and S. Guha, *Phys. Rev. A* **95**, 012304 (2017).
- [45] R. Czupryniak, E. Chitambar, J. Steinmetz, and A. N. Jordan, *Phys. Rev. A* **106**, 032424 (2022).
- [46] S. Guha, H. Krovi, C. A. Fuchs, Z. Dutton, J. A. Slater, and others, *Phys. Rev. A* (2015).
- [47] P. Dhara, A. Patil, H. Krovi, and S. Guha, *Phys. Rev. A* **104**, 052612 (2021).
- [48] P. Dhara, D. Englund, and S. Guha, *Phys. Rev. Res.* **5**, 033149 (2023).
- [49] Y. Lee, E. Bersin, A. Dahlberg, S. Wehner, and D. Englund, *npj Quantum Information* **8**, 1 (2022).
- [50] I. Padilla, A. Sajjad, B. N. Saif, and S. Guha, Unpublished (2024).
- [51] C. W. Helstrom, *Quantum Detection and Estimation Theory* (Academic Press, New York, 1976).
- [52] H. Yuen and J. Shapiro, *IEEE Transactions on Information Theory* **24**, 657 (1978).
- [53] J. Rehacek, M. Pařr, B. Stoklasa, Z. Hradil, and L. L. Sánchez-Soto, *Opt. Lett.* **42**, 231 (2017).
- [54] L.-M. Duan and H. J. Kimble, *Phys. Rev. Lett.* **92**, 127902 (2004).
- [55] M. Pařr, B. Stoklasa, Z. Hradil, L. L. Sánchez-Soto, and J. Rehacek, *Optica* **3**, 1144 (2016).
- [56] The proof that the pairwise measurement with 2-dimensional apertures attains the QFI is beyond the scope of this work and will be shown in a future publication.
- [57] D. Gottesman and I. L. Chuang, arXiv preprint [quant-ph/9908010](https://arxiv.org/abs/quant-ph/9908010) (1999).